Halogen Nuclear Quadrupole Coupling Constants in Non-axially symmetric Molecules; *Ab initio* Calculations, which Include Correlation, Compared with Experiment*

Michael H. Palmer and John A. Blair-Fish[a]

Department of Chemistry, University of Edinburgh, West Mains Road, Edinburgh EH9 3JJ, Scotland, UK.
[a] Computing Service, University of Edinburgh, Mayfield Road, Edinburgh EH9 3JZ, Scotland, UK.

Z. Naturforsch. **53a,** 370–382 (1998); received March 24, 1998

Ab initio determination of the electric field gradient (EFG) tensors at halogen and other centres enabled determination of the nuclear quadrupole coupling constants (NQCC) for a diverse set of C_{2v}, C_{3v} and other symmetry molecules of general formula MH_2X_2 and MHX_3, where the halogen atoms (X) are Cl, Br and I, and the heavy central atoms (M) are C and Si. The study presents results at a standardised level of calculation, triple-zeta in the valence space plus polarisation functions (TZVP) for the equilibrium geometry stage; all-electron MP2 correlation is included in all these studies. For the bromo and iodo compounds, especially the latter, it is essential to allow core polarisation, by decontraction of the p,d-functions. This is conveniently done by initial optimization of the structure with a partly contracted basis, followed by reestablishment of the equilibrium structure with the decontracted basis.

The NQCCs, derived from the EFGs, using the 'best' values for the atomic quadruple moments Cl, Br and I, lead to good agreement with the inertial axis (IA) data obtained from microwave spectroscopy. When the data from the present study is plotted against the values derived from the IA data, obtained by whatever approximations chosen by the MW authors, we obtain a linear regression for the data (85 points) with the slope 1.0365 and intercept –0.1737, with standard errors of 0.0042 and 0.2042, respectively; these are statistically identical results irrespective of whether the data is restricted to IA or EFG principal axis (PA) data.

Since as in the C_{3v} MH_3X compounds studied previously, a close correlation of the microwave spectral data with the calculations was observed using the 'best' current values for Q_Z, there seems no need to postulate that the values of Q_{Br} for both ^{79}Br and ^{81}Br are seriously in error. A scaling downwards of Q_Z by about 5% for Br and I increases the agreement with experiment, but the contributions of relativistic effects are unknown, and could lead to further reassessment.

Of the two common assumptions used in MW spectroscopy, to convert from IA to EFG-PA data, either (a) cylindrical symmetry of the NQCC along the bond direction, or (b) coincidence of the tensor principal element with the bond axis, the latter is found to be a much more realistic approximation.

1. Introduction

In previous papers of this series, [1] [2] [3] [4], we have studied a range of molecules containing various quadrupolar nuclei, and most recently this was axially symmetric halogen-containing compounds of both organic and inorganic types [5]. The present paper continues this last aspect, but relates to the non-axially symmetric compounds, especially organic compounds of C_{2v} and C_{3v} symmetry such as CH_2X_2 and HCX_3, together with their silane analogs. These studies concern individual molecules at equilibrium. Microwave spectroscopy (MW) for gaseous molecules leads to data directly comparable with the present results. However, the MW determined are a result purely of the set of atomic masses, and are not connected with the equilibrium structure and its electronic wavefunction except via the atomic numbers of the nuclei, so that IA data alone is of limited value.

In the low symmetry cases such as C_{2v} and C_s, the asymmetry parameter (η) is nonzero. In the normal convention for NQCCs, the magnitudes are given by: $\chi_{zz} \geq \chi_{yy} \geq \chi_{xx}$; the asymmetry parameter (η) is given by $(\chi_{xx} - \chi_{yy})/\chi_{zz}$; this limits the upper value of η to unity, since the Laplace relationship also obtains, i.e. the sum of the NQCCs is zero. The microwave spectroscopic definition of asymmetry parameter is different, and this can lead to values greater than unity; if the molecules is an oblate top, the axis identities are $z = c$, $x = a$, $y = b$; if it is a prolate top, $z = a$, $x = b$, $y = c$, where a, b, c are the inertial axes.

NQR has been widely used for studies of halogenated compounds, but because of the 3/2 and 5/2 nuclear spin,

---

* Presented at the XIVth International Symposium on Nuclear Quadrupole Interactions, Pisa, Italy, July 20–25, 1997.

Reprint requests to Dr. M. H. Palmer; Fax: +44 131-650-4743.

0932-0784 / 98 / 0600-0370 $ 06.00 © – Verlag der Zeitschrift für Naturforschung, D-72027 Tübingen

only the resonance frequencies (ν) can be determined from polycrystalline samples (1); the asymmetry parameter (η) requires the use of a single crystal or other techniques [6]. Much of the early (largely NQR) literature has been reviewed by Lucken [6]; however, it is appropriate to note the correlations between ^{81}Br NQR frequencies and Hammett sigma constants [7].

NQR Frequency for 3/2–1/2 Transition:

$$\nu = \frac{e^2 Q q_{zz}}{2h}(1+\eta^2/3)^{1/2}. \tag{1}$$

As a typical example, the ^{35}Cl NQR frequency for methyl chloride at 77 K is 34.029 MHz, to be compared with 37.3767 MHz for the study at room temperature [8] [9]. The effect is both one of temperature and lattice effects. Indeed, analysis of the NQR frequency and molar heat capacity against temperature lead to the value of –2.870(330) MHz as the crystalline contribution to the observed frequency at 0 K [10]. In most cases, we will refer to the MW data if available, while NQR data, which contains the condensed phase effects, will be used in the absence of MW data. In this and the following sections, experimental claimed errors in the last digits are in parentheses, and the quadrupole coupling data refer to the isotopes ^{35}Cl, ^{79}Br and ^{127}I; data for the other isotopes can be obtained by scaling of the results by ratio of the atomic quadrupole moments.

2. Coordinate Transformations for Quadrupole Coupling

First we note some of the approximations which are commonly used in MW spectroscopy in order to transform the coordinate system of the NQCC tensor from EFG-IA to EFG-PA systems. The case considered is where there is a plane of symmetry, leading to C_s symmetry for the system. One of the diagonalised tensor values is unchanged between the IA and EFG-PA systems, so that the principal values obtained are dependent on the accuracy of the (least-well determined) off-diagonal element, χ_{ab}, whose sign is unknown. If χ_{ab} is not determined, progress can still be made. Given the angle θ_a between the a-axis and the C-halogen bond is known from the substitution structure, a very common approach is (a) to assume that the z-axis lies along the C-halogen bond direction. Hence here $\theta_a = \theta_{za}$. Alternatively, (b) it is assumed that the EFG-PA tensor has cylindrical symmetry, whereby $\chi_{zz} = -2\chi_{xx} = -2\chi_{yy}$ where the c-axis is unchanged in the plane of symmetry case. This last method immediately gives χ_{zz} from $-2\chi_{cc}$.

In the present study, we perform *ab initio* calculation of the EFGs (q_{ij}) at the centre of interest in the molecule, and convert this tensor to the NQCC tensor (χ_{ij}) by means of (2) and (3) [11]. The SCF or MP2 wave-function is denoted by ψ_0.

The diagonalised tensor values (χ_{ii}) in MHz compare directly with the MW experimental NQCC in the EFG-PA system. If the molecule has a plane of symmetry, the c-axis is perpendicular to the plane, and if this coincidences with the EFG x-PA, then the components along the inertial axes a, b are as shown in (4). Hence having evaluated χ_{ii} we can determine the components of the IA tensor elements using these equations and a knowledge of the angle between the EFG-PA and the IA, here θ_{za}.

Typical diagonal and off-diagonal Electric Field Gradient Operators:

$$\begin{aligned} q_{zz} &= \left\langle \psi_0 \middle| (3z^2 - r^2)/r^5 \middle| \psi_0 \right\rangle, \\ q_{xy} &= \left\langle \psi_0 \middle| (3xy)/r^5 \middle| \psi_0 \right\rangle. \end{aligned} \tag{2a, b}$$

Nuclear Quadrupole Coupling Constant and Electric Field Gradient:

$$\chi_{ii} = e^2 Q_Z q_{ii}/h = 234.96\, Q_Z q_{ii}. \tag{3}$$

Rotation from EFG-PA to IA Data in Molecules with a Plane of Symmetry:

$$\begin{aligned} &\chi_{aa} = \chi_{yy}\sin^2\theta_{za} + \chi_{zz}\cos^2\theta_{za}, \\ &\chi_{bb} = \chi_{yy}\cos^2\theta_{za} + \chi_{zz}\sin^2\theta_{za}, \\ &\chi_{cc} = \chi_{xx}, \\ &2\chi_{ab} = [\chi_{aa} - \chi_{bb}]\tan 2\theta_{za}, \\ &\chi_{yy}[\sin^2\theta_{za} - \cos^2\theta_{za}] = \\ &[\chi_{aa}\sin^2\theta_{za} - \chi_{bb}\cos^2\theta_{za}], \\ &\chi_{zz}[\cos^2\theta_{za} - \sin^2\theta_{za}] = \\ &[\chi_{aa}\cos^2\theta_{za} - \chi_{bb}\sin^2\theta_{za}]. \end{aligned} \tag{4a–f}$$

2.1. Basis Sets and Theoretical Methods

The theoretical methods are the same as in [5] and do not require much amplification here. The Huzinaga/Dunning triple zeta valence (TZV) type [12] were extended by polarisation functions [13]; some other larger elements were from our own bases and are described more fully [14] [15]. However, it was found that while the bromine and iodine bases of Huzinaga [16] [17] with total functions 14s11p5d (Br) contracted to s/p/d terms

Table 1. Total energies and EFG for alkyl halides; TZVP + MP2 method.

Compound	Symm.	Energy/a.u.	q_{zz}	q_{yy}	q_{xx}	α
EtCl	C_s	−538.71731	−3.5293	1.7836	1.7456	0.700
i-PrCl	C_s	−577.93654	−3.4211	1.7304	1.6906	0.683
t-BuCl	C_{3v}	−617.15732	−3.3760	1.6880	1.6880	0.000
CH_2Cl_2	C_{2v}	−958.58856	−3.8879	2.0514	1.8364	0.854
$HCCl_3$	C_{3v}	−1417.70418	−4.0451	2.0234	2.0216	1.190
CCl_4	T_d	−1876.79865	−4.1446	2.0723	2.0723	0.000
CF_2Cl_2	C_{2v}	−1156.81274	−3.9006	1.9709	1.9296	1.274
CH_2FCl	C_s	−598.59930	−3.5319	1.9283	1.6035	
1,1-$C_3H_4Cl_2$	C_{2v}	−1035.80868	−3.7978	1.9674	1.8302	
EtBr	C_s	−2651.67247	−7.2838	3.6852	3.5977	
EtBr(ext)	C_s	−2651.93198	−7.3973	3.7454	3.6511	0.769
i-PrBr	C_s	−2690.89117	−7.0246	3.5484	3.4752	0.686
i-PrBr(ext)	C_s	−2691.15066	−7.1412	3.6040	3.5363	0.686
t-BuBr	C_s	−2730.11158	−6.9035	3.4518	3.4518	0.000
t-BuBr(ext)	C_s	−2730.37105	−7.0278	3.5139	3.5139	0.000
CH_2Br_2(ext)	C_{2v}	−5184.51452	−7.9518	4.1499	3.8011	0.114
$HCBr_3$(ext)	C_{3v}	−7756.21755	−9.3029	4.6515	4.6515	
CBr_4(ext)	T_d	−10328.61938	−8.8462	4.4236	4.4236	0.000
CH_2BrCl	C_s	−3071.55848	−3.7929(Cl)	2.0000	1.7929	1.189
CH_2BrCl	C_s	−3071.55848	−7.8685(Br)	4.1240	3.7436	0.678
CH_2BrCl(ext)	C_s	−3071.81798	−3.7959(Cl)	2.0002	1.7956	
CH_2BrCl(ext)	C_s	−3071.81798	−7.9875(Br)	4.1787	3.8079	0.678
EtI	C_s	−6994.30297	−7.2380	3.6367	3.5980	0.903
EtI(ext)	C_s	−6995.58537	−10.4735	5.2645	5.2058	
i-PrI	C_s	−7033.52365	−7.009	3.5575	3.4401	0.840
i-PrI(ext)	C_s	−7034.80563	−10.1266	5.1409	4.9824	
t-BuI	C_{3v}	−7072.74673	−6.9177	3.4588	3.4588	0.000
t-BuI(ext)	C_{3v}	−7074.02807	−10.0080	3.4589	3.4589	0.000
CH_2I_2	C_{2v}	−13869.78140	−8.0672	4.0857	3.9782	
HCI_3	C_{3v}	−20784.45302	−8.5707	4.3613	4.2061	
CI_4	T_{3d}	−27699.12684	−9.1668	4.5834	4.5834	0.000
CH_2ClI	C_s	−7417.18647	−3.8259(Cl)	1.9690	1.8568	
CH_2ClI	C_s	−7417.18647	−7.9541(I)	4.1019	3.8489	1.044
CH_2ClI(ext)	C_s	−7415.46897	−3.8282(Cl)	1.9714	1.8566	1.202
CH_2ClI(ext)	C_s	−7415.46897	−11.4944(I)	5.9260	5.5651	1.044

[611111111/611111/411], and 18s14p8d (I) contracted to [3322212111/3332111/4211], respectively, led to very acceptable structural parameters, this was not true of the quadrupole coupling at ^{127}I in particular, with ^{79,81}Br being only marginally acceptable. It was necessary to decontract the bromine p-functions further to [311111111], while the iodine basis above required the addition of further terms of each of s,p,d-type, the p-set becoming [321111111111]; if this was not done, then HI had the dipole reversed from the expected direction. Because of the high degree of decontraction of these orbitals, the molecular total energies are very good, and since the heavy atoms contribute a very high proportion of the total energy, are relatively close to the Hartree-Fock limiting values for these molecules.

In summary, the equilibrium geometries were obtained with the semi-contracted sets shown; the equilibrium geometries were then re-established with the full decontracted sets, and the wave-functions saved as Natural Orbitals (NOs). Reoperation of the optimization mode for the latter, facilitiates storage of the NO for subsequent analysis. All of the calculations were performed with the **GAMESS-UK** quantum chemistry package [18] [19]. In the Atomic Units energy scale, 1 a.u. = 2626 kJmol^{-1}.

2.2. Atomic Quadrupole Moments

The present set of nuclei has nuclear spin $I = 3/2$ (^{35}Cl, ^{37}Cl, ^{79}Br, and ^{81}Br), $I = 5/2$ (^{127}I). The individual NQCCs, with standard deviations in parentheses are: ^{35}Cl (−81.65(80) mb) and ^{37}Cl (−64.35(64) mb); less well determined [20] are the values for the ^{79}Br, ^{81}Br and ^{127}I isotopes which have Q_Z +331(4), +276(4); −789 mb, respectively [21] [22]. These values will be used for conversion of field gradients EFG/a.u. to NQCC/MHz via (3). The EFG to NQCC conversion ratios are: ^{35}Cl: 1 a.u. = −19.184484 MHz; ^{79}Br 1 a.u. = 77.77176 MHz; ^{127}I 1 a.u. = −185.38344 MHz.

3. Results and Discussion

Tables 1–2 show the compounds studied by the above standardised methods, and include total energies (a.u.), symmetries and EFGs (a.u.). The first stage is determination of the equilibrium structure and the corresponding IA system, and comparison with experiment. All molecular properties such as NQCC are evaluated for the equilibrium structure. In the present paper we do not discuss the equilibrium structures in great detail, choosing to take a few typical examples from different symmetry classes. The rotation constants *A*, *B*, *C* (MHz) are shown in Table 3; these give a clear measure of the overall structure comparison with experiment, and hence show that the IAs lie in similar positions in the theoretical equilibrium structure and in the substitution structure from the MW analysis. As implied, we are primarily concerned with the halogen atoms being connected to a tetravalent centre in the present study.

The EFGs are converted to the NQCC using the above conversion factors, and are compared with the IA quadrupole data, as shown in Tables 4–7. Where NQR data is entered, this is purely for completeness, since the varied temperatures and assumptions of zero asymmetry, consistent with the time of investigations (circa 1960), are such that no direct comparison of the data is possible.

The Tables are completed by ones relating to electron distribution, Mulliken populations and comparison with experimental dipole moments (Tables 8 and 9).

Table 2. Total energies and EFG for silyl halides; TZVP + MP2 method.

Compound	Symm.	Energy/a.u.	q_{zz}	q_{yy}	q_{xx}
H_3SiCl	C_{3v}	−750.65672	−2.0648	1.0324	1.0324
H_2SiCl_2	C_{2v}	−1209.84228	−2.0108	1.0833	0.9274
$HSiCl_3$	C_{3v}	−1668.99126	−2.0468	1.0268	1.0199
$SiCl_4$	C_{3d}	−2128.15537	−2.1598	1.0799	1.0799
$MeSiH_2Cl$	C_s	−789.88841	−1.9503	0.9847	0.9655
Me_2SiHCl	C_s	−829.12017	−1.8702	0.9405	0.9297
Me_2SiCl_2	C_{2v}	−1288.29377	−1.9042	0.9931	0.9111
Me_3SiCl	C_{3v}	−868.35242	1.8093	0.9046	0.9046
H_3SiBr(ext)	C_{3v}	−2863.86902	−4.6585	2.3288	2.3288
H_2SiBr_2	C_{2v}	−5435.72868	−4.5608	2.4388	2.1221
$MeSiH_2Br$	C_s	−2903.10075	−4.3716	2.2079	2.1637
Me_2SiHBr	C_s	−2942.07292	−4.0930	2.0533	2.0387
Me_3SiBr	C_{3v}	−2981.30514	−3.9347	1.9669	1.9669
H_3SiI(ext)	C_{3v}	−7207.50302	−7.3766	3.6866	3.6866
H_3SiI(diff)	C_{3v}	−7207.63100	−6.7867	3.3917	3.3917
$MeSiH_2I$	C_s	−7246.86358	−6.3513	3.167	3.1313

Table 3. Rotation constants (MHz) for alkyl and silyl halides.

Compound	Method	*A*	*B*	*C*
EtCl	Calc.	31642.0	5472.0	4952.8
	MW[23]	31337.35	5493.69	4962.30
EtBr	Calc.	30324.0	3787.2	3513.9
	MW[27]	29955.61	3804.0	3522.9
EtI	Calc.	29787.0	3081.0	2891.8
	MW[31]	29116.33	2979.57	2796.45
CH_2Cl_2	Calc.	32345	3258.2	3017.0
	MW[33]	32001.8	3320.4	3065.2
CH_2Br_2	Calc.	26305	1215.8	1170.9
	MW[35]	26031.31.8	1238.54	1190.94
CH_2FCl	Calc.	42186	5640.6	5141.2
	MW[43]	41811.2	5716.0	5194.9
CH_2BrCl	Calc.	29367.0	2096.4	1981.5
	MW[42]	29198.34	2133.14	2012.90
CH_2ICl	Calc.	28518	1626.4	1553.7
	MW[44][45]	27418.8	1622.0	1545.8
CF_2Cl_2	Calc.	4102.1	2597.0	2202.8
	MW[40]	4118.90	2638.70	2233.72
i-PrCl	Calc.	8152.3	4559.6	3215.7
	MW[49]	8086.09	4570.82	3207.57
i-PrBr	Calc.	8123.2	2902.7	2292.2
	MW[46][47]	8038.89	2917.75	2295.33
i-PrI	Calc.	8179.5	2266.2	1879.7
	MW[48][47]	8022.08	2187.18	1817.67
t-BuCl	Calc.	4581.1	3023.4	3023.4
	MW[59][53]		3017.69	3017.72
t-BuBr	Calc.	4579.6	2042.9	2042.9
	MW[50][55]		2044.24	2044.24
t-BuI	Calc.	4610.2	1619.6	1619.6
	MW[55]		1560.60	1560.60
$HCCl_3$	Calc.	3251.9	3251.9	1686.9
	MW[38]	3302.41	3302.41	
1,1-$C_3H_4Cl_2$	Calc.	3995.5	2875.8	1933.2
	MW[39]	3981.86	2919.19	1949.41
H_2SiCl_2	Calc.	14078	2512.8	2187.6
	MW[63]	14135.01	2573.58	2232.61
$HSiCl_3$	Calc.	2425.2	2425.2	1300.8
	MW[65]	2472.47	2472.47	
Me_2SiCl_2	Calc.	2562.8	1800.8	1604.5
	MW[69]	2584.14	1842.51	1628.64
$MeSiH_2Cl$	Calc.	15946	3848.4	3281.0
	MW[67][58]	16077.9	3904.4	3325.6
$MeSiH_2I$	Calc.	14405	1871.1	1706.3
	MW[67][68]	14747.84	1893.50	1728.52

3.1. Structure and Inertial Axes for Alkyl and Silyl Halides

The ethyl halides (Et-X, X = Cl, [23] [24] Br, [28] [25] [26] [27] I, [29] [30] [31]) have been analysed by MW spectroscopy in terms of the trans-conformer, and hence C_s symmetry. The 3-fold rotor axis of the methyl-group is slightly offset from the C-C bond axis in all cases. All three molecules have a very similar position in the inertial axis frame, namely the halogen and trans-H_β effectively on the *a*-axis, and the pair of $CH_{2\beta}$-$CH_{2\alpha}$ groups in the positive and negative *b*-axes, respectively. Experimentally, the NQCCs evaluated here are the

Table 4. Alkyl chloride quadrupole coupling constants (MHz) compared with experiment.

Compound	Method	χ_{zz}	χ_{yy}	χ_{xx}	η
EtCl	MP2	–67.708	+33.488	+34.219	0.0108
EtCl	MW[23][24]	–68.84	+35.64	+33.2	0.0354
EtCl	NQR[7]	(–)65.518(av)	(+)32.759	(+)32.759	0.0(ass)
EtCl	MP2	–49.729(aa)	+15.509(bb)	+34.219(cc)	0.4303
EtCl	MW[23][24]	–49.29(9)(aa)	+14.15(12)(cc)	+35.64(12)(cc)	0.4360
i-PrCl	MP2	–65.632	+33.197	+32.435	0.0116
i-PrCl	MW[49]	–67.82(12)	+34.843	+32.977	0.0275
i-PrCl	NQR[7]	(–)63.878	(+)31.939	(+)31.939	0.0(ass)
i-PrCl	MP2	–59.080(aa)	+33.197(cc)	+25.882(bb)	0.1238
i-PrCl	MW[49]	–61.49(11)(aa)	+34.81(25)(bb)	+26.68(25)(cc)	0.1322
t-PrCl	MP2	–64.767	+32.383	+32.383	0.0000
t-PrCl	MW[60]	–67.56(50)	+33.78(50)	+33.78(50)	0.0000
t-PrCl	MW[54][53]	–67.12(32)	+33.56(32)	+33.56(32)	0.0000
CH_2Cl_2	MP2	–74.588	+35.231	+39.355	0.0553
CH_2Cl_2	MW[33]	–78.4(20)	+39.2(10)	+39.2(10)	0.876
CH_2Cl_2	NQR[7]	(–)72.982	(+)35.991	+35.991	0.0(ass)
CH_2Cl_2	MP2	–39.355(aa)	+3.224(bb)	+39.355(cc)	0.8485
CH_2Cl_2	MW[33]	–41.8(10)(aa)	+2.6(10)(bb)	+39.2(10)(cc)	0.876
CH_2FCl	MP2	–67.757	+36.994	+30.762	0.0920
CH_2FCl	MW[43]	–74.30(187)	+39.059(18)	+35.20(186)	0.0519
CH_2FCl	MP2	–50.746(aa)	+13.751(bb)	+36.994(cc)	0.4538
CH_2FCl	MW[43]	–52.570(aa)(26)	+13.469(bb)(20)	+39.059(cc)(18)	0.4868
CH_2BrCl	MP2	–72.765	+38.368	+34.395	0.0546
CH_2BrCl	MW[42]	–75.19	+39.43	+35.76	0.0488
CH_2BrCl	MP2	–34.852(aa)	–3.523(bb)	+38.373(cc)	0.9049
CH_2BrCl	MW[42]	–33.64(70)(aa)	–5.79(41)(bb)	+39.43(81)(cc)	0.7063
CH_2ClI	MP2	–73.441	+37.821	+35.619	0.0300
CH_2ClI	MW[44][45]	–74.7(19)	+40.1(12)	+34.6(22)	0.0736
CH_2ClI	MP2	–32.708(aa)	–5.114(bb)	+37.821(cc)	0.7296
CH_2ClI	MW[44][45]	–31.1(11)(aa)	–9.0(6)(bb)	+40.1(12)(cc)	0.5511
CF_2Cl_2	MP2	–74.831	+37.811	+37.018	0.0106
CF_2Cl_2	MW[40][41]	–80.37(30)	+41.65(25)	+38.71(22)	0.0366
CF_2Cl_2	MP2	–41.938(aa)	+4.917(bb)	+37.018(cc)	0.0106
CF_2Cl_2	MW[40][41]	–43.42(16)(aa)	+4.70(20)(bb)	+38.71(22)(cc)	0.0366
$HCCl_3$	MP2	–77.604	+38.818	+38.784	0.0048
$HCCl_3$	NQR[38]	(–)76.508	(+)38.254	(+)38.254	0.0(ass)
$HCCl_3$	MP2	+29.145(aa)			
$HCCl_3$	MW[38][57]	+28.54(3)(aa)			
CCl_4	MP2	–79.512	+39.756	+39.756	0.0000
CCl_4	NQR[7]	(–)81.28	(+)40.32	(+)40.32	0.0(ass)
$C_3H_4Cl_2$	MP2	–72.858	+37.744	+35.112	0.0361
$C_3H_4Cl_2$	MW[39]	–76.4(3)	+39.445(5)	+37.0(3)	0.0320
$C_3H_4Cl_2$	MP2	–41.874(aa)	++4.128(bb)	+37.744(cc)	0.8027
$C_3H_4Cl_2$	MW[39]	–43.545(5)(aa)	+4.100(5)(bb)	+39.445(5)(cc)	0.8117

sum and difference terms, $\chi^+ = -\chi_{aa} = \chi_{bb} + \chi_{cc}$ and $\chi^- = \chi_{bb} - \chi_{cc}$, respectively. The isopropyl halides show many features similar to the ethyl halides. The *a*-axis lies close to the halogen and the bisector of the C-C-C angle.

Next we briefly refer to some examples of the mixed dihalogenomethanes, since these cases show higher asymmetry parameters than the above. Dichloromethane is a typical case [33]; the calculated rotation constants (*A*, *B*, *C*) in MHz are shown in Table 3. These are typical levels of agreement between the equilibrium geometriy rotation constants (for the most common isotopes) and the substitution structure in MW spectroscopy. These data yield the bond lengths (*A*) and angles (degr.) (experimental in parentheses) H-C 1.0804 (1.068(5)), C-Cl 1.7735 (1.7724(5)) and C-C-Cl 112.94 (111.8(1)), respectively. Since the two structure determinations are not expected to be identical, this is good agreement. In this C_{2v} symmetry example, the *b*-axis bisects the Cl-C-Cl angle, with the *a*-axis parallel to the Cl-Cl axis but displaced towards C.

Of the C_{2v} symmetry systems, CF_2Cl_2 is a typical case. The present equilibrium structure shows bonds and angles, with MW determinations in parentheses, C-Cl

Table 5. Alkyl bromide and iodide quadrupole coupling constants (MHz) compared with experiment.

Compound	Method	χ_{zz}	χ_{yy}	χ_{xx}	η
CH_2Br_2	MP2	+618.427	322.742	–295.614	0.0439
CH_2Br_2	MW [36] [37]	+595.74	–310.28	–285.46	0.0417
CH_2Br_2(ext)	MP2	+364.848 (aa)	–37.354 (bb)	–327.423 (cc)	0.7950
CH_2Br_2	MW [36] [35] [37]	+335.21 (42) (aa)	–24.93 (24) (bb)	–310.28 (48)	0.8513
CH_2BrCl	MP2	+621.203	–324.984	–296.149	0.0464
CH_2BrCl	MW [42]	+591.23	–307.53	–283.70	0.0403
CH_2BrCl	MP2	–410.388 (aa)	–85.330 (bb)	–325.062 (cc)	0.0820
CH_2BrCl	MW [42]	–383.33 (59) (aa)	–75.80 (37) (bb)	–307.53 (69) (cc)	0.6045
CH_2ClI	MP2	–2130.873	+1098.579	+1031.683	0.0314
CH_2ClI	MW [45]	–1999.0 (29)	+1029.3 (21)	+969.7 (35)	0.0298
CH_2ClI	MP2	–1542.998 (aa)	+443.807 (bb)	+1098.579 (cc)	0.3741
CH_2ClI	MW [45]	–1421.9 (aa) (19)	+392.6 (bb) (10)	+1029.3 (cc) (21)	0.4471
EtBr	MP2	+566.472	–286.603	–279.800	0.0120
EtBr	MW [27]	+544.03 (168)	–273.71 (17)	–270.32 (166)	0.0062
EtBr	MP2	+446.769 (aa)	–155.413 (bb)	–279.800 (cc)	0.3041
EtBr	MW [27]	+417.75 (20) (aa)	–144.05 (17) (bb)	–273.71 (cc) (17)	0.3104
EtI	MP2	–1941.618	+975.945	+965.061	0.0056
EtI	MW [29] [31]	–1815.22 (85)	+913.50 (26)	+901.71 (81)	0.0065
EtI	MP2	–1572.144 (aa)	+975.945 (cc)	+596.199 (bb)	0.2415
EtI	MW [31]	–1478.06 (39) (aa)	+913.50 (26) (cc)	+564.555 (32) (bb)	0.2361
i-PrBr	MP2	+555.385	–280.289	–275.026	0.0094
i-PrBr	MW [46]	+514.2 (5)	–264.890 (5)	–249.310 (5)	0.0303
i-PrBr	MP2	+512.079 (aa)	–280.289 (bb)	–231.719 (cc)	0.0948
i-PrBr	MW [46] [47]	+480.02 (27) (aa)	–265.10 (72) (bb)	–214.92 (27) (cc)	0.0146
i-PrI	MP2	–1877.311	+953.938	+923.662	0.0156
i-PrI	MW [48]	–1742.1	+883.7	+858.4	0.0145
i-PrI	MP2	–1747.931 (aa)	+749.272 (cc)	+923.662 (bb)	0.0740
i-PrI	MW [48] [47]	–1626.36 (49) (aa)	+742.56 (98) (cc)	+883.81 (98) (bb)	0.0868
t-BuBr	MP2	+546.560	–273.281	–273.281	0.0000
t-BuBr	MW [50]	+513.7 (8)	–256.85 (8)	–265.85 (8)	0.0000
t-BuI	MP2	–1855.308	+641.219	+641.219	0.0000
$HCBr_3$	MP2	+723.505	–361.753	–361.753	0.0000
CBr_4	MP2	+687.985	–344.034	–344.034	0.0000
CBr_4	NQR [6]	(+)641.32 (av)	(–)320.66	(–)320.66	0.0 (ass)
HCI_3	MP2	–1588.860	+808.509	+779.739	0.0181
HCI_3	NQR [62]	(–)2028.15	(+)1014.407	(+)1014.07	0.0500
CI_4	MP2	–1699.367	+849.683	+849.683	0.0000
CI_4	NQR [62]	(–)2128.74	(+)1064.37	(+)1064.37	0.0260

1.7686 (1.744), C-F 1.3348 (1.345), Cl-C-Cl 112.0 (112.5) and F-C-F 107.8 (106.2), respectively [40]. Of these differences, the C-Cl one is surprisingly large; in general we would expect bond differences of about 0.01 Å.

If we take the fluorochloromethane case, the symmetry is reduced to C_s; here the corresponding data for A, B, C is within 1% of experiment [43]. The a-axis again lies close to the F-Cl direction but tilted slightly towards C, such that the Cl atom lies almost on the a-axis. This is a situation where the determination of substitution coordinates is most unreliable. However, the agreement between the equilibrium and (assumed) substitution structure is again good; namely C-F 1.3654 (1.370) C-Cl 1.7794 (1.7621) and F-C-Cl 110.4 (110.1). When we turn to bromochloromethane, the rotation constants, A, B, C are again in excellent agreement, and the molecular dimensions are in agreement with the experimentally assumed structure, with C-Br 1.9421 (1.930), C-Cl 1.7748 (1.769), C-H 1.0800 (1.074), Br-C-Cl 113.0 (112.3). For iodochloromethane we have A, B, C and an equilibrium structure very similar to the assumed experimental one [44] [45]. In this instance, the I-atom lies effectively on the a-axis, which cuts the C-Cl bond relatively close to the Cl atom. The general level of agreement between the EFG-IA data and that found experimentally [45], is again fairly satisfactory. The off-diagonal element (χ_{ab}) whose sign cannot be determined experimentally, is clearly positive for this molecule.

In general, the silane structures are also in good agreement with the substitution structures from the MW investigations, but the differences are often larger than in the corresponding alkane molecules. For example, the

Table 6. Halogenosilane quadrupole coupling constants (MHz) compared with experiment.

Compound	Method	χ_{zz}	χ_{yy}	χ_{xx}	η
H_2SiCl_2	MP2	–38.576	+20.782	+17.792	0.0755
H_2SiCl_2	MW [63] [64]	–38.33 (13)	+20.7245 (19)	+17.60 (13)	0.0815
H_2SiCl_2	MP2	–21.304 (aa)	+0.520 (bb)	+20.782 (cc)	0.9511
H_2SiCl_2	MW [63] [64]	–20.4150 (19) (aa)	–0.3095 (19) (bb)	+20.7245 (cc)	0.9702
$HSiCl_3$	MP2	–39.266	+19.699	+19.565	0.0034
$HSiCl_3$	NQR [7]	–37.834	+18.917	+18.917	0.0 (ass)
$HSiCl_3$	MP2	+13.785 (cc)	–33.353 (bb)	+19.565 (aa)	–3.8386
$HSiCl_3$	MW [66]	+13.66 (15) (cc)	–34.49 (bb)	+20.83 (aa)	–4.05
$SiCl_4$	MP2	–41.435	+20.717	+20.717	0.0000
$SiCl_4$	NQR [7]	–40.731 (av)	+20.365	+20.365	0.0 (ass)
$MeSiH_2Cl$	MP2	–37.416	+18.891	+18.523	0.0098
$MeSiH_2Cl$	MW [58]	–37.65	+18.63	+19.02	
$MeSiH_2Cl$	MP2	–28.036 (aa)	+9.143 (bb)	+18.891 (cc)	0.3477
Me_2SiCl_2	MP2	–36.531	+19.051	+17.478	0.0430
Me_2SiCl_2	MW [69]	–38.0 (16)	+23.2	+14.8	0.22
Me_2SiCl_2	MP2	–18.929 (aa)	+19.051 (cc)	–0.124 (bb)	0.9871
Me_2SiCl_2	MW [69]	–19.6 (3) (aa)	+23.4 (14) (cc)	–3.7 (14) (bb)	0.6824
$MeSiH_2I$	MP2	–1177.421	+596.325	+580.485	0.0135
$MeSiH_2I$	MW [67] [68]	–1157.21 (63)	+587.31 (26)	+569.90 (54)	0.0150
$MeSiH_2I$	MP2	–1030.215 (aa)	+596.325 (cc)	+433.279 (bb)	0.1583
$MeSiH_2I$	MW [68]	–1012.65 (43) (aa)	+587.31 (26) (cc)	+425.35 (37) (bb)	0.1599
Me_3SiCl	MP2	–34.711	+17.355	+17.355	0.0000
Me_3SiCl	MW [61]	–46.9 (15)	+23.45	+23.45	0.0000

Table 7. Linear correlations between calculated and observed NQCC (MHz).

Correlation	Slope (m)	Intercept (*c*)	SE (slope)	SE (Intercept)	CC	NP
Chloro (IA)	1.0385	–0.1894	0.0056	0.2617	0.9993	51
Chloro (PA)	1.0391	–0.0691	0.0047	0.2508	0.9994	61
Chloro (IA+PA)	1.0365	–0.1737	0.0042	0.2042	0.9993	85
Bromo (IA+PA)	0.9501	0.6156	0.0023	1.1343	0.9999	43
Iodo (IA+PA)	0.9414	0.6360	0.0037	5.5927	0.9996	48

C_{2v} dichlorosilane molecule has dimensions (compared with experiment in parentheses) Si-Cl 2.0523 (2.33 (3)), Si-H 1.4627 (1.480 (15)), Cl-Si-Cl 110.20 (109.7 (3)) and H-Si-H 113.17 (111.3 (3)) [63]. In the case of dichlorodimethylsilane, the difference (calc./obs.) in angles C-Si-C (115.1 / 114.7) and Cl-Si-Cl (107.9 / 107.2) is well brought out, but the bond lengths are less in agreement, with Si-C (1.8573 / 1.845) Si-Cl (2.0709 / 2.055) [69]; the NQCC are not in such good agreement for this molecule either.

Methyliodosilane has been studied in detail by MW spectroscopy [67] [68]. Like iodoethane, the I atom lies close to the *a*-axis, with the *b*-axis bisecting the Si-C bond. The angle θ_{za} is calculated to be 16.8° in exact agreement with the value obtained experimentally. Thus the structure is in good agreement with experiment. The major bond lengths are (calc./obs.): Si-I 2.4751 (2.444), Si-C 1.8674 (1.857), Si-H 1.4721 (1.460), I-Si-C 108.5 (108.8).

3.2. Quadrupole Coupling Constants in Relation to Structure

The ethyl halides provide the simplest non-axial symmetry cases; in the case of chloroethane, the difference in the two assumptions of (a) either zero asymmetry to enable the conversion of IA to EFG-PA data, or (b), assuming the EFG-PA to lie along the bond axis leads to results for the χ_{zz} of –71.28 MHz and –68.84 MHz, respectively [24]. The present data shows that the angle between the EFG-PA and the bond direction is 0.70°, and hence the second assumption is the more reasonable, with data as shown in Table 4. There is good agreement between the IA data and the present study for chloroethane, with similar angle θ_{za} 24.929 (compared with 26.9 from the averaged experimental data) [24]. For both bromo- and iodo-ethane, the off-diagonal NQCC element χ_{ab} was determined, hence allowing the diagnonalisation of the tensor, and the EFG-PA to be determined without the assumptions for the chloro-compound. Again, the present results are in good agreement with experiment [29] [31]. We find the asymmetry parameter for this series of compounds to be small (Et-X, η 0.0108 (X = Cl), 0.0128 (X = Br) and 0.0056 (X = I). However, the better assumption of (a) and (b) above, is that the EFG-PA lies along the C-X bond. Overall there is pleasing agreement between the observed and calculated IA data in this set of compounds.

Table 8. Comparison of dipole moments with experiment.

Compound	Dipole moment (Calc)	Dipole moment (Obs)	Reference
MeCl	2.022	1.892(1)	[74]
MeBr	2.013	1.797(15)	[80] [27]
MeI	1.720	1.618	[80] [31]
EtCl	2.115	2.101	[75]
EtBr	1.988	1.85	[75]
EtI	1.7201	1.77(10)	[56]
i-PrCl	2.1462	2.04	[60]
i-PrBr	2.0832	2.04	[60]
i-PrI	1.7906	1.94	[60]
CF_3Cl	–0.525	(–)0.50(1)	[80]
CF_3Br	–0.672	(–)0.639(2)	[79]
CF_3I	–0.962	(–)1.048(3)	[79]
t-BuCl	2.144	2.13, 2.18	[54] [76]
t-BuBr	2.081	2.24	[76]
t-BuI	1.761	1.60	[34]
H_2CCl_2	1.751	1.62(2)	[80]
$C_3H_4Cl_2$	2.040	1.58	[39]
H_2SiCl_2	1.561	1.13(2)	[63]
$MeSiH_2Cl$	2.059	1.935(20)	[67]
$MeSiH_2Br$	2.220	1.841(20)	[67]
$MeSiH_2I$	1.823	1.952(20)	[67]
H_3SiCl	1.705	1.303(10)	[80] [77]
H_3SiBr	1.625	1.319(8)	[78]
H_3SiI	1.389	1.62	[77]
Me_3SiCl	2.319	2.13	[76]
Me_3SiBr	2.349	2.28	[76]
H_3Ge	2.581	2.124(20)	[80]
F_3SiI	–1.4267	–1.11	[72]
F_3SiBr	–1.0341	–0.835	[72]
F_3SiCl	–0.7299	–0.636	[72]
HCl	1.432	1.12(4)	[80]
HBr	1.076	0.83(2)	[80]
HI	0.798	0.445(20)	[80]
HCCBr	0.1890	0.22962(1)	[51] [52]

Table 9. Mulliken atomic populations at equilibrium structure.

EtCl	Cl 17.1285	C_α 6.2144	C_α 6.3723	H_β 0.8470
	H_β 0.8703	H_β 0.8604		
i-PrCl	Cl 17.1299	C_2 6.1093	H_2 0.8380	$C_{1,3}$ 6.3746
	H_{3av} 0.8623			
t-BuCl	Cl 17.1305	C 6.0360	C_{Me} 6.3659	H_{3av} 0.8596
CH_2Cl_2	Cl 17.0526	C 6.2663	H 0.8142	
EtBr	Br 35.1336	C_α 6.2141	C_β 6.3620	H_α 0.8491
	H_β 0.8708	H_β 0.8607		
i-PrBr	Br 35.1419	C_2 6.1019	$C_{1,3}$ 6.3663	H_2 0.8470
	H_{ip} 0.8493	H_{oop} 0.8646		
t-BuBr	Br 35.1480	C(Br) 6.0349	C 6.3588	H 0.8601
EtI	I 52.8871	C_α 6.5472	C_β 6.3539	H_α 0.8145
	$H_{\beta(av)}$ 0.8609			
t-BuI	I 52.8745	C(I) 6.4294	C 6.3339	H 0.8549
CH_2FCl	Cl 17.0966	F 9.2042	C 5.9900	H 0.8546
CH_2Cl_2	Cl 17.0526	C 6.2663	H 0.8142	
H_2SiCl_2	Si 13.3368	Cl 17.2447	H 1.0869	
$MeSiH_2Cl$	H_{Me} 0.8386	C 6.6427	Si 13.3302	H_{Si} 1.1148
$MeSiH_2Br$	H_{Me} 0.8382	C 6.6337	Si 13.3337	H_{Si} 1.1102
	Br 35.2976			
$MeSiH_2I$	H_{Me} 0.8317	C 6.6318	Si 13.4348	H_{Si} 1.0899
	I 5.2583			
Me_2SiHCl	H_{Me} 0.8407	C 6.6456	Si 13.2615	H_{Si} 1.1205
	Cl 17.2827			
F_3CCl	Cl 17.0307	C 5.5436	F 9.1419	
F_3CBr	Br 35.0304	C 5.5691	F 9.1335	
F_3CI	I 52.9649	C 5.6426	F 9.1308	

The present data correctly represents the experimental correlation of NQCC against structure for the series of chloromethanes, CH_nCl_{4-n}, $n = 0-4$ first exhibited by Lucken (Fig. 10.1 in [6]). Here we show the corresponding EFG-PA data against a term representing the number of halogen atoms (Figure 1). A similar relationship occurs for the bromo- and iodo-compounds.

For iodochloromethane [44] [45], the I-atom lies effectively on the *a*-axis, which cuts the C-Cl bond relatively close to the Cl atom. The general level of agreement between the EFG-IA data and that found experimentally [45], is again fairly satisfactory. The off-diagonal element (χ_{ab}) whose sign cannot be determined experimentally, is clearly positive for this molecule.

Of the trihalogeno-methanes and -silanes, there is only MW data for chloroform [38] [57] and trichlorosilane [65] [66]. In these C_{3v} molecules, the 3-fold *z*-axis identifies with the *c*-axis in MW spectroscopy, leading to the *a*- and *b*-axes being degenerate. This arises from the difinition of the principal axes of inertia, being $I_a \le I_b \le I_c$. Here there is three symmetrically placed quadrupoles about the *z*-axis, and none of the EFG-PA lie along the *x*, *y*, *z* (or *a*, *b*, *c*)-coordinate systems. Thus if η is defined as $(q_{zz} - q_{yy})/q_{zz}$, there are no immediate limits to η. If cylindrical symmetry is assumed, the current state of this art for the trichloro-compounds, then the EFG-PA components along the *z*-axis are $eQq\cos\alpha$ where α is the Cl-M-Cl angle. This simplifies to a value for η being close to $(1 - \cos\alpha)/\cos\alpha$. Potential confusion with the EFG-PA values can occur; thus for chloroform, the IA data yields $eQV_{zz} = eQq_{cc} = +28.54(3)$ MHz [57]. The assumption of axial charge symmetry, leads to the EFG-PA data –80.39(22) MHz, also confusingly cited as eQV_{aa} [38]. A further feature of unusual type, is that the haloform and trihalogenosilane molecules show very high asymmetry parameters when referred to the IA frame; thus for chloroform [57], we have $\eta = (q_{aa} - q_{bb})/q_{cc} = -3.74(4)$ as a typical example. For the trichlorosilane it is even larger (–4.05) [66]. In practice, we find the asymmetry parameters low around the Cl centres in both molecules, so that the above (expediently chosen) analysis is a reasonable approximation. In Table 4–6, we also show the (approximate) NQR EFG-PA values for these and related molecules, which would have been obtained by the assumption of local EFG cylindrical symmetry; again the data are all consistent. In particular, the fact that the EFG-PA values of the NQCC at ^{35}Cl in the silanes when compared with the methanes, are nearly half the magnitudes, emerges.

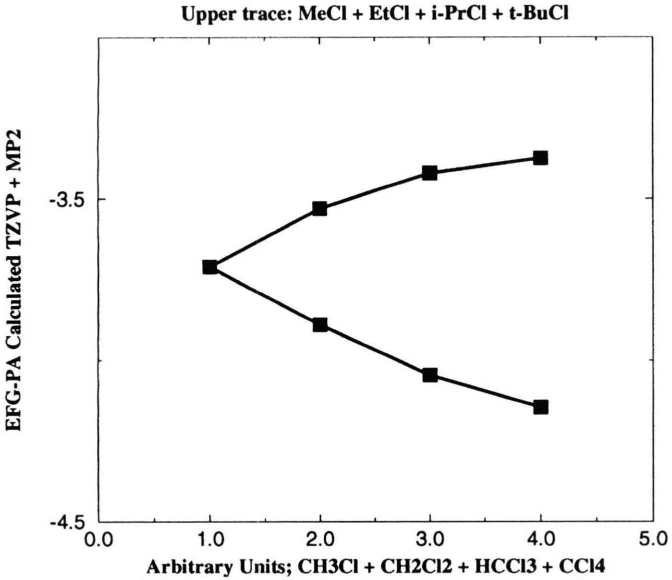

Fig. 1. ^{35}Cl EFG -PA for halogenomethanes versus numbers of halogens.

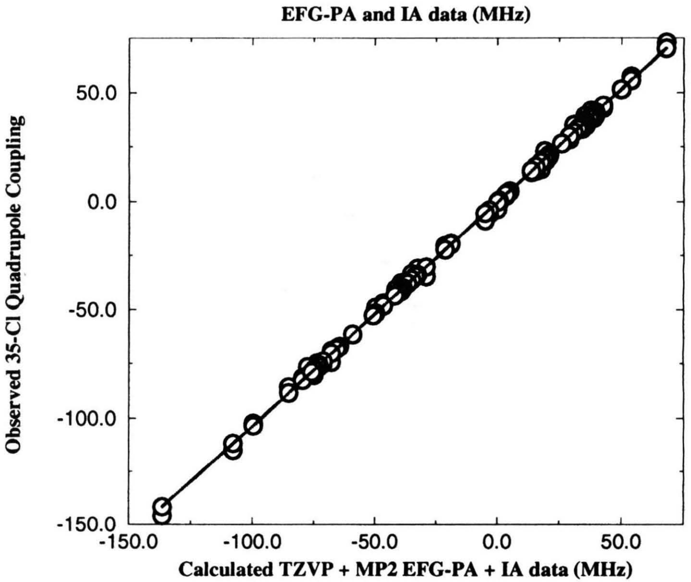

Fig. 2. ^{35}Cl quadrupole coupling calculation versus experiment.

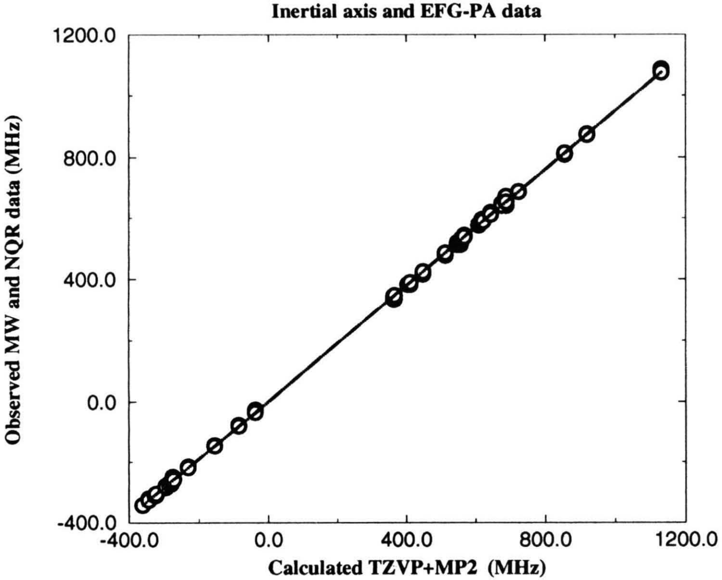

Fig. 3. ^{79}Br quadrupole coupling calculation versus experiment.

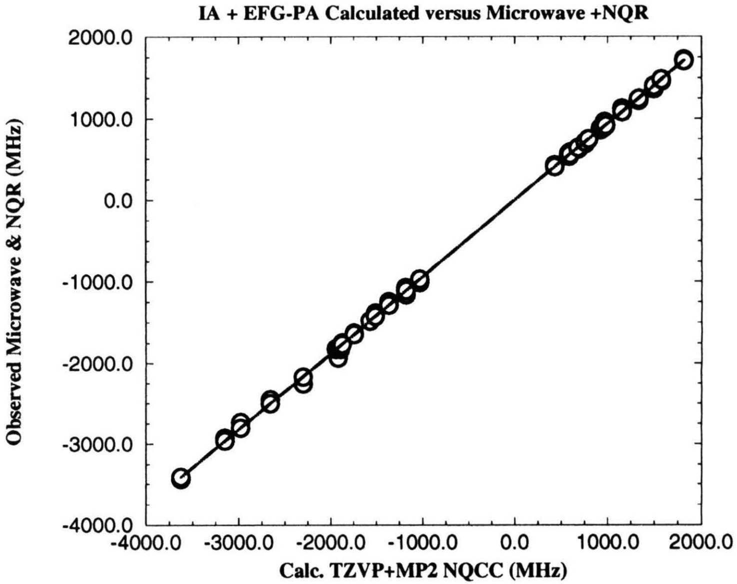

Fig. 4. ^{127}I quadrupole coupling calculation versus experiment.

The MW study of dimethyldichlorosilane [69], leads to a much higher η for the EFG-PA results than found here; the value seems high by comparison with other molecules, but again (in the absence of determination of the off-diagonal elements) cylindrical asymmetry was assumed. The only other discrepancy appears to be trimethylsilyl chloride, where the axially symmetric molecule leads to χ_{zz} –34.711 MHz in the present study compared with –46.9(15) MHz in an early MW study [61]. These data have omitted from the correlations shown, since it seems unlikely that the present calculations, which are consistent with the other silyl results, could be in error to such a large degree. There are problems with internal rotation in the analyses of spectra from such compounds.

3.3. EFG and Derived Quadrupole Coupling Constants in Relation to Experiment

In Table 7, we show the slope (*m*), intercept (*c*) for a series of correlations $y = mx + c$, where *y* is the Observed NQCC, and *x* is the Calculated NQCC. The correlation coefficient (CC), and Standard Errors (SE) of slope and intercept for N-sets (NP) of data are shown. Figure 2 shows the overall correlation of the ^{35}Cl quadrupole coupling constants, calculated versus experiment for the IA data. Since the methods used are identical with those for the axially-symmetric compounds of our previous paper [5], we include these compounds; the IA and PA data are identical in these latter cases. Thus the correlation, over some 51 points contains both organic and inorganic compounds, and in the latter case, contains halogens and inter-halogens, as well as the silyl compounds. The corresponding data for the bromo and iodo compounds is shown in Fig. 3 and Fig. 4. In each case, the fit is very satisfactory, all data are effectively controlled by scatter, and no systematic or specific mis-matches are seen.

If the EFG-PA data from the present study is plotted against the values derived from the IA data, by whatever approximations chosen by the MW authors, but especially (a) cylindrical symmetry or (b) *z*-axis coincident with bond axis, and (c) after determination of the off-diagonal elements, and direct determination of the EFG-PA results, we obtain an almost identical correlation. In this instance, the corresponding linear regression data for the slope and intercept are statistically identical results to the IA results, showing the high level of agreement between theoretical and experimental data. Thus the intrinsic errors in the theoretical data, namely non-idential structures, and hence differing moments of inertia and inertial axis positioning, and the errors in the experimental data, including the claimed errors (shown in the Tables), as well as the approximations (a) and (b) above, all balance out.

4. Implications for the Atomic Quadrupole Moments

We have performed correlations of the above type for a number of years [1]. However, whilst these show the degree of scatter between the calculated and observed data, the Laplace relationship, $\chi_{xx} + \chi_{yy} + \chi_{zz} = 0$, makes it inevitable that the correlation lines will pass close to the origin. In order to determine the ‘effective atomic quadrupole coupling constants’ for each halogen, we scale the values used by the slope of the correlation line. This gives the values, Cl –84.63(33), Br +314.48(80), I –724.74(310) mb, where the errors are based on the SE of the regression slope. The % changes for the nuclei are thus Cl +3.6, Br –5.0 and I –5.9% respectively. The primary factors which may distort these values are (i) whether the basis sets and methodology used are returning a constant proportion of the EFG, (ii) whether there are relativistic effects, which will increase with the atomic number of the element. We cannot be sure of either of these factors. However, there seems no need to reassess the value for the ^{79}Br nucleus downwards by 10%, as has recently been suggested on the basis of calculations on brominechloride (BrCl) [70]. Our previous paper [5] shows that the present adjustment in the value of $Q_{^{79}\mathrm{Br}}$ of –5.0% would give effectively exact agreement with experiment for BrCl. The reason for the discrepancies in the ‘effective atomic quadrupole coupling constants’ required for calibration of EFG calculations with large elements such as Br and I, is the essential need to (i) operate with a large atomic basis set, and then (b) to decontract the gaussian orbitals to almost the maximum degree, in order to allow core polarisation to be possible in molecular cases [5].

5. Electric Charge Distributions

5.1. Dipole Moments

We now report the dipole moment results obtained and compare these with those from various experimental methods. Although there are compendia of dipole moments for simple compound such as the present series [7], the values obtained over the rather narrow range, by diverse methods show considerable scatter for individual compounds, and there is no Stark effect MW studies on a number of key compounds; new data is urgently awaited. The individual components in the inertial axes may cause some problems since the MW intensity varies with the square of the dipole moment. Ethyl iodide is typical with μ_a 1.75(5) and μ_b 0.25(1) D [80]. The ratio of 7:1 in the components shows that the intensity of the separate spectra would differ by 49:1. We assign a positive sign to the dipole moment to mean that the negative end of the dipole lies towards the quadrupolar halogen under study. In order to widen the range of data, we include some of the compounds from our previous study [5]. The overall correlation of the data shown provides a linear correlation of form $\mu_{\text{Expt}} = 0.906\ \mu_{\text{Calc}} + 0.036$. The SE in slope is 0.025, and intercept 0.043, with a correlation coefficient of 0.9865 for 37 compounds. In general the correlation is satisfactory, but the uncertain validity of some of the experimental (solution) data to the present correlation makes detailed discussion impracticable. However, it appears that the dipole moments in the series: Me, Et, i-Pr and t-Bu increase slowly for all individual halogens, while the Me-X series with X = Cl, Br and I decrease [60]. These effects are consistent with the electron donating effects of alkyl groups, and electron acceptance of all halogens relative to an attached C-atom. In the case of the CF_3-X and SiF_3-X compounds, the dipole moments are of different sign to the above. Thus vector addition of the F_3 atoms in an approximately tetrahedral environment, leads to one F-C or F-Si dipole along the internuclear principal axis; this is more than sufficient to outweight the C-Cl and Si-Cl dipoles in the opposite direction, so that the MF_3-X system behaves like an extended interhalogen, with F at the negative end of the dipole [32]. In this way, the lower dipole moments of the CF_3-X relative to the CH_3-X series are readily explained [79], as is the fact that the CF_3-X series have dipole moments $I > Br > Cl$, contrasting with CH_3-X which are in the reverse order, while the trifluorosilyl halides have almost identical dipole moments to the trifluoromethyl halides [72] [73].

5.2. Atomic Populations by Mulliken Analyses

Finally, we analyse the electronic charge distribution in terms of Mulliken atomic populations, and the individual bond components. For the chloroalkanes, the bond dipoles comprising the difference in total atomic populations relative to the free atom sums in the atomic groupings, show that H-C bonds are polarised $H^{\delta+}$-$C^{\delta-}$ with δ about 0.154e, except in isopropyl-compounds where the H-C-Cl is more polarised (0.162e). The methyl groups are fairly constant electron denors by about 0.040e to adjacent C-Cl; the C-Cl bond dipole is about 0.130e. In the bromo-compounds, the C-Br polarisation is about 0.134e, effectively the same as in the chloro-compounds. In contrast, the alkyl iodides have the C-I bond dipole reversed to the C-halogen ones above, with the I atom losing about 0.109e; thus the dipole moment of iodomethane arises from the H-C bond polarisation outweighing the C-I one. The presence of more than one halogen leads to each having a smaller total population than separately, with the H-C dipole acting as the electronic balance. Thus dichloromethane has H-C dipoles of 0.185e, slightly increased over the monochloro-compound, but the C-Cl dipoles are reduced to 0.053e. The C atom in CH_2BrCl is very similar in total charge to that in CH_2Cl_2, but CH_2FCl has a nearly neutral C atom, with high bond dipole on C-F but nearly typical C-Cl bond. In the case of the halogenosilanes, the H-Si bonds are polarised in the sense $H^{\delta-}$-$Si^{\delta+}$, where δ is 0.286e (Cl), 0.297e (Br) and 0.055e (I). Thus the iodine atom in iodosilane is negative in contrast to iodomethane molecule. The d-orbital populations in all these simple silanes are variable but low in every case. There is no evidence to connect the quadrupole coupling constants with d-orbital participation. The principal reason for the NQCC at halogen being nearly halved in the silanes compared with the methane series was covered in our previous paper.

6. Conclusions

Overall there is pleasing agreement between the observed and calculated IA data in this set of compounds. The angle θ_a between the *a*-axis and the C-halogen bond known from the substitution structure, leads to either (a) the assumption that the *z*-axis lies along the C-halogen bond direction. Hence here $\theta_a = \theta_{za}$. Alternatively, (b) it is assumed that the EFG-PA tensor has cylindrical symmetry, whereby $\chi_{zz} = -2\chi_{xx} = -2\chi_{yy} = -2\chi_{cc}$; in this case, the *c*-axis component is unchanged in the plane of symmetry case. This last method immediately gives χ_{zz} from $-2\chi_{cc}$.

With the advent of Fourier transform MW spectrometers, the higher resolution by a factor of 40 in some cases, leads to the determination of the off-diagonal elements (χ_{ab} etc) directly. The removal of the necessity for assumptions (a) or (b) above, can lead to marked differences. Thus for dichlorosilane, the EFG-PA value changes from –42.0 MHz ($\eta = 0.0$ assumed) to –38.33 MHz (with $\eta = 0.0815$), a nearly 10% change [64]. As it turns out, this improves the agreement with the present calculations.

We find the asymmetry parameter for the alkyl halide series of compounds to be small; typical values in the ethyl halides are: Et-X, η 0.0108 (X = Cl), 0.0128 (X = Br) and 0.0056 (X = I). However, the better assumption of (a) and (b) above, is that the EFG-PA lies along the C-X bond.

The electric dipole moments are reasonably well correlated with experimental data, but the absence of some Stark measurements has meant the need to utilise some solution data. The charge distributions as determined by Mulliken analyses are consistent with the dipole moments, and in particular the signs of the dipole moments are standardised, and these correlations make the differences and similarities of CF_3 and SiF_3 series of compounds in relation to the CH_3 and SiH_3 series better understood.

Acknowledgements

We thank the SERC (now EPSRC) for purchase of a DEC AXP Alpha 3600 work-station, and Edinburgh University for the generous provision of time on the Cray T3D computer.

[1] M. H. Palmer, Z. Naturforsch. **41a**, 147 (1986).
[2] M. H. Palmer, Z. Naturforsch. **45a**, 357 (1990).
[3] M. H. Palmer, Z. Naturforsch. **47a**, 203 (1992).
[4] M. H. Palmer, Z. Naturforsch. **51a**, 442 (1995).
[5] M. H. Palmer, Z. Naturforsch. **53a**, 383 (1998).
[6] E. A. C. Lucken, "Quadrupole Coupling Constants", Acad. Press, New York 1969, Chapt. 10, p. 167 *etseq.*
[7] H. O. Hooper and P. J. Bray, J. Chem. Phys. **33**, 334 (1960).
[8] S. G. Kukolich and A. C. Nelson, J. Chem. Phys. **57**, 4052 (1972).
[9] S. G. Kukolich and A. C. Nelson, J. Amer. Chem. Soc. **95**, 680 (1973).
[10] G. A. Monti, C. A. Martin, D. Rupp, and E. A. C. Lucken, J. Phys. C; Solid State Phys. **21**, 3023 (1988).
[11] R. Moccia and M. Zandomeneghi, Adv. Nucl. Quadrupole Reson. **2**, 135 (1975).
[12] T. H. Dunning, J. Chem. Phys. **55**, 716 (1971).
[13] R. Ahlrichs and P. R. Taylor, J. Chim. Phys. **78**, (1981) 315.
[14] M. H. Palmer, J. Molec. Structure **405**, (1997) 179–191.
[15] M. H. Palmer, J. Molec. Structure **405**, (1997) 193–205.
[16] S. Huzinaga, J. Chem. Phys. **66**, 4245 (1977).
[17] S. Huzinaga, J. Chem. Phys **71**, 1980 (1979).
[18] M. Dupuis, D. Spangler, and J. Wendoloski, "NRCC Software Catalog", Vol. 1, Program No. QG01 (GAMESS), 1980.
[19] M. F. Guest, J. Kendrick, J. H. van Lenthe, K. Schoeffel, and P. Sherwood, "GAMESS-UK: User's Guide and Reference Manual", Version 5, December 1995, CFS Ltd. EPSRC Daresbzury Laboratory.
[20] P. Pyykko, Z. Naturforsch. **47a**, 189 (1992).
[21] G. H. Fuller, J. Phys. Chem. Ref. Data **5**, No. 4, 835 (1976).
[22] P. Raghaven, Atomic Data and Nuclear Data Tables, Acad. Press, New York 42, 189 (1989).
[23] R. H. Schwendeman and G. D. Jacobs, J. Chem. Phys. B36, 1245f (1962).
[24] M. Hayashi and T. Inagusa, J. Molec. Structure **220**, 103 (1990).
[25] W. Zeil and D. Christen, J. Phys. Chem. **84**, 1790 (1980).
[26] J. Gripp, H. Dreizler, and R. Schwarz, Z. Naturforsch. **40a**, 575 (1985).
[27] T. Inagusa and M. Hayashi, J. Molec. Spectrosc. **129**, 160 (1988).
[28] C. Flanagan and L. Pierce, J. Chem. Phys. **38**, 2963 (1963).
[29] D. Boucher, A. Dubrelle, and J. Demaison, J. Molec. Spectrosc. **84**, 375 (1980).
[30] J. Gripp and H. Dreizler, U. Naturforsch, **43a**, 971 (1988).
[31] T. Inagusa, M. Fujitake, and M. Hayashi, J. Molec. Spectrosc. **128**, 456 (1988).
[32] E. A. C. Lucken, Quadrupole Coupling Constants, Acad. Press, New York 1969, Chapt. 12, p. 288 *etseq.*
[33] R. J. Myers and W. D. Gwinn, J. Chem. Phys. **20**, 1420 (1952).
[34] C.-Y. Chen and R. J. W. LeFevre, J. Chem. Soc. 40 (1966).
[35] R. W. Davis and M. C. L. Gerry, J. Molec. Spectrosc. **109**, 269 (1985).
[36] D. Chadwick and D. J. Millen, Trans. Faraday Soc. **67**, 1551 (1971).
[37] Y. Niide, H. Tanaka, and I. Ohkoshi, J. Molec. Spectrosc. **120**, 11 (1990).
[38] P. N. Wolfe, J. Chem. Phys. **25**, 976 (1956).
[39] W. H. Flygare, A. Narath, and W. D. Gwinn, J. Chem. Phys. **36**, 200 (1962).
[40] H. Takeo and C. Matsumura, Bull. Chem. Soc. Japan **50**, 636 (1977).
[41] E. L. Beeson and C. F. Su, J. Chem. Phys. **66**, 330 (1977).
[42] Y. Niide and I. Ohkoshi, J. Molec. Spectrosc. **136**, 17 (1989).
[43] S. Blanco, A. Lesarri, J. C. Lopez, J. L. Alonso, and A. Guarnieri, J. Molec. Spectrosc. **174**, 397 (1995).
[44] I. Ohkoshi, Y. Niide, and M. Takano, J. Molec. Spectrosc. **124**, 118 (1987).
[45] I. Ohkoshi and Y. Niide, J. Molec. Spectrosc. **126**, 282 (1987).
[46] R. H. Schwendeman and F. L. Tobiason, J. Chem. Phys. **43**, 201 (1965).
[47] C. Ikeda, T. Inagusa, and M. Hayashi, J. Molec. Spectrosc. **135**, 334 (1989).
[48] P. Groner, Y. S. Li, and J. R. Durig, J. Molec. Spectrosc. **72**, 20 (1978).
[49] F. L. Tobiason and R. H. Schwendeman, J. Chem. Phys. **40**, 1014 (1964).
[50] A. C. Legon, D. J. Millen, and A. Samsam-Baktiari, J. Molec. Struct. **52**, 71 (1979).
[51] A. P. Porter and P. D. Godfrey, J. Molec. Spectrosc. **68**, 492 (1977).
[52] S. M. Bass, R. L. DeLeon, and J. S. Muenter, J. Chem. Phys. **92**, 71 (1990).

[53] J. H. Carpenter, R. Crane, and J. G. Smith, J. Molec. Spectrosc. **141**, 91 (1990).

[54] D. R. Lide and M. Jen, J. Chem. Phys. **38**, 1504 (1963).

[55] S. Brotherton, A. C. Legon, J. C. Thorn, B. Turner, A. L. Wallwork, J. H. Carpenter, E. Johnson, and J. G. Smith, J. Chem. Soc. Faraday trans. **89**, 397 (1993).

[56] T. Kasuya and T. Oka, J. Phys. Soc. Japan **15**, 296 (1960).

[57] J. H. Carpenter, P. J. Seo, and D. H. Whiffen, J. Molec. Spectrosc. **170**, 215 (1995).

[58] W. Zeil, Selected. Topics Molec. Phys., Proc. Int. Conf. 1970 (publ. 1972), Ed. E. Clementi, p.103–113.

[59] W. Zeil, M. Winnewisser, and K. Muller, Z. Naturforsch. B16a, 1250 (1961).

[60] W. Zeil, M.Winnewisser, and W. Plein, Z. Naturforsch. **17a**, 823 (1962).

[61] J. R. Durig, R. O. Carter, and Y. S. Li, J. Molec. Spectrosc. **44**, 18 (1972).

[62] S. I. Gushchin, S. A. Petukhov, E. V. Bryukhova, and G. K. Semin, Izv. Akad. Nauk SSSR, Ser. Shim., No. 8, 1920 (1983).

[63] R. W. Davis and M. C. L. Gerry, J. Molec. Spectrosc. **60**, 117 (1976).

[64] K. D. Hensel, W. Jager, M. C. L. Gerry, and I. Merke, J. Molec. Spectrosc. **158**, 131 (1993).

[65] H. Takeo and C. Matsumura, Bull. Chem. Soc. Japan **50**, 1633 (1977).

[66] J. H. Carpenter and J. G. Smith, J. Molec. Spectrosc. **121**, 270 (1987).

[67] M. Fujitake, J. Nakagawa, and M. Hayashi, J. Molec. spectrosc. **119**, 367 (1986).

[68] M. Hayashi, M. Fujitake, and K. Kishioka, J. Molec. Spectrosc. **135**, 305 (1989).

[69] M. Nakata, H. Takeo, and C. Matsumura, J. Molec. Spectrosc. **82**, 117 (1980).

[70] P. W. Fowler, S. A. Peebles, A. C. Legon, and A. J. Sadlej, Chem. Phys. Letters **257**, 249 (1996).

[71] A. L. McClellan, Tables of Experimental Dipole Moments, W. H. Freemen, San Francisco 1963.

[72] A. P. Cox. T. R. Gayton, and C. A. Rego, J. Molec. Structure **190**, 419 (1988).

[73] A. P. Cox, I. C. Ewart, and T. R. Gaydon, J. Molec. Spectrosc. **125**, 76 (1987).

[74] J. P. DeJongh and H. A. Dijkerman, J. Molec. Spectrosc. **25**, 129 (1968).

[75] M. Hayashi, M. Fujitake, T. Inagusa, and S. Miyazaki, J. Molec. Structure **216**, 9 (1990).

[76] S. Sorriso, A. Ricci, and R. Danieli, J. Organomet. Chem. **87**, 61 (1975).

[77] J. M. Bellama and A. G. McDiarmid, J. Organomet. Chem **24**, 91 (1970).

[78] K. F. Doessel and D. H. Sutter, U. Naturforsch. **32a**, 1444 (1977).

[79] A. P. Cox, G. Duxbury, J. A. Hardy, and Y. Kawashima, J. Chem. Soc. Faraday II **76**, 339 (1980).

[80] W. Gordy and R. L. Cook, Microwave Molecular Spectra Wiley-Intersci. New York 1970, p. 349–361.